Cell Reports

Report

Early Developmental Program Shapes Colony Morphology in Bacteria

Graphical Abstract

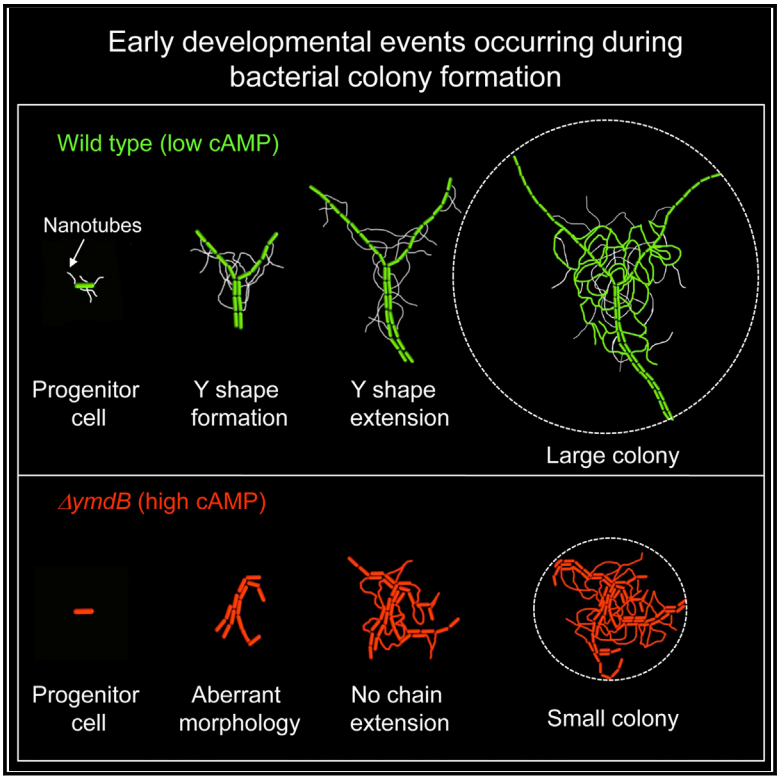

Highlights

- Highly ordered spatiotemporal events occur during bacterial colony development
- Colony typically initiates by formation of leading-cell chains arranged in a Y shape
- Y-arm extension defines the size and the shape of the future colony
- A mutant in the phosphodiesterase *ymdB* displays aberrant developmental patterns

Authors

Gideon Mamou, Ganesh Babu Malli Mohan, Alex Rouvinski, Alex Rosenberg, Sigal Ben-Yehuda

Correspondence

sigalb@ekmd.huji.ac.il

In Brief

Mamou et al. show that a sequence of hierarchical spatiotemporal events occurs during colony initiation by the bacterium *Bacillus subtilis*. Utilizing laser-induced ablations, they demonstrate that the size and shape of the future colony relies on these primary deterministic events. Furthermore, they identify molecular cues directing this developmental process.

Mamou et al., 2016, Cell Reports *14*, 1850–1857
March 1, 2016
http://dx.doi.org/10.1016/j.celrep.2016.01.071

CellPress

OPEN ACCESS
CellPress

Cell Reports
Report

Early Developmental Program Shapes Colony Morphology in Bacteria

Gideon Mamou,[1] Ganesh Babu Malli Mohan,[1] Alex Rouvinski,[1,2] Alex Rosenberg,[1] and Sigal Ben-Yehuda[1,*]
[1]Department of Microbiology and Molecular Genetics, Institute for Medical Research Israel-Canada, The Hebrew University-Hadassah Medical School, POB 12272, The Hebrew University of Jerusalem, 91120 Jerusalem, Israel
[2]Present address: Unité de Virologie Structurale, Département de Virologie, Institut Pasteur, 25-28 Rue du Dr Roux, 75015 Paris, France
*Correspondence: sigalb@ekmd.huji.ac.il
http://dx.doi.org/10.1016/j.celrep.2016.01.071

SUMMARY

When grown on a solid surface, bacteria form highly organized colonies, yet little is known about the earliest stages of colony establishment. Following *Bacillus subtilis* colony development from a single progenitor cell, a sequence of highly ordered spatiotemporal events was revealed. Colony was initiated by the formation of leading-cell chains, deriving from the colony center and extending in multiple directions, typically in a "Y-shaped" structure. By eradicating particular cells during these early stages, we could influence the shape of the resulting colony and demonstrate that Y-arm extension defines colony size. A mutant in *ymdB* encoding a phosphodiesterase displayed unordered developmental patterns, indicating a role in guiding these initial events. Finally, we provide evidence that intercellular nanotubes contribute to proper colony formation. In summary, we reveal a "construction plan" for building a colony and provide the initial molecular basis for this process.

INTRODUCTION

During the course of colony formation, a single bacterium divides to create a colony composed of billions of its descendants organized in a remarkable ordered structure. These massive cell divisions are associated with secretion of various molecules, comprising the extracellular matrix, essential for establishing a proper colony structure (Ben-Jacob and Levine, 2006; Branda et al., 2005; Flemming et al., 2007). Bacterial colonies display distinct properties such as size, color, shape, and texture, which fundamentally vary among different species. These features were the basic means for identifying, classifying, and characterizing bacteria in the early days of microbiology (Kaufmann and Schaible, 2005) and are presently still exploited for clinical and research applications. Formation of bacterial colonies is a constructive survival strategy, enabling bacteria to utilize a greater variety of nutrients, endure rapid environmental changes, and resist antibiotic threats (Christensen et al., 2002; Lewis, 2001; Moons et al., 2009).

Colony formation and maintenance require coordinated communal activities to benefit colony members. Such remarkable coordination is exemplified by the Gram-negative bacterium *Myxococcus xanthus*, which employs social motility to swarm, predate, and build organ-like spore filled fruiting bodies (Kaiser, 2006; Mauriello and Zusman, 2007; Zhang et al., 2012). Similarly, cells of the Gram-positive bacterium *Paenibacillus dendritiformis* utilize swarming to develop complex colonial branching patterns. Interestingly, it has been demonstrated that secretion of a sibling lethal factor serves to direct colony growth and morphology of these elaborated structures (Be'er et al., 2009). In the soil bacterium *Bacillus subtilis*, mature colonies display a high degree of spatiotemporal organization that was found to be affected by genes involved in motility, matrix production, and sporulation, highlighting the complexity of colony architecture (Branda et al., 2001, 2004, 2006; Kearns et al., 2005).

Despite the fact that analysis of bacterial colonies began decades ago, relatively little is known about the earliest stages of colony formation. Furthermore, factors limiting colony size and expansion are largely unrevealed. Here, we show that a sequence of hierarchical spatiotemporal events occurs during colony initiation by *B. subtilis*. Moreover, by utilizing laser induced ablations, we demonstrate that the size and shape of the future colony relies on these primary deterministic events. Finally, we identified molecular cues directing this developmental process.

RESULTS

Early Stages of Colony Development Exhibit Characteristic Morphological Patterns

To examine the initial stages of colony establishment, we designed a chamber (Figures S1A and S1B) to image a colony as it develops from a single progenitor cell into a three dimensional (3D) structure, utilizing confocal laser scanning microscopy (CLSM). Inspecting the early stages of colony formation revealed that subsequent to a lag phase, the progenitor cell divides to create elongated chains that are typically arranged in a "Y-like" shape (Figure 1A). A closer examination revealed that the founder cell initially generates a linear elongated chain of ~10–15 cells. The cell chain then tends to split in the middle, such that the cells adjacent to the break point are pushed

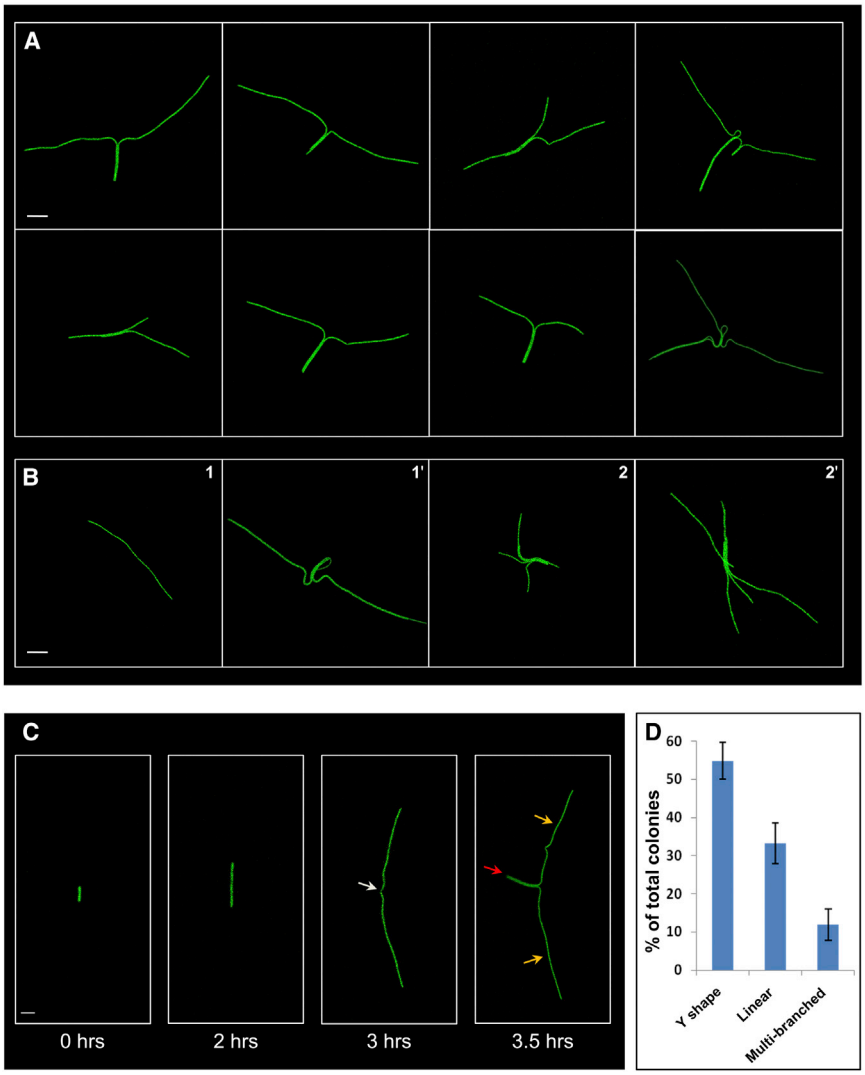

Figure 1. Early Morphological Patterns of Developing Colonies

(A) Fluorescence images of typical Y-shaped structures observed at t = 3–4 hr during colony formation by AR16 (P_{rrnE}-*gfp*) cells.

(B) Fluorescence images of linear (1, 1′) and multi-branched (2, 2′) structures, observed at t = 2.5 hr (1, 2) and subsequently at t = 4 hr (1′, 2′) during colony formation by AR16 cells.

(C) Fluorescence images of initial chain branching and Y-shape formation of AR16 developing colony at the indicated time points. White arrow points to the position of chain breakage, and yellow and red arrows indicate single- and double-chained Y arms, respectively.

(D) Frequency of each of the initial morphologies described above (A and B), as calculated from 11 separate experiments. The total colony number was 272.

Scale bars represent 5 μm.

perpendicularly to the original chain layout. This breakage ultimately produces a third, double-chained Y arm (Figure 1C; Movie S1). Notably, similar initial stages were apparent when the colony developed from a single dormant spore (Figure S1C), implying that this pattern persists even when the establishing cell resides in an entirely different physiological state. Statistical analysis of colony initiation patterns (n = 272) revealed that ~55% initiated with a Y shape (Figure 1D). The second common motif was a linear shape, in which the initial chain remained unbroken, and ~10% of the colonies exhibited multibranched forms (Figures 1B and 1D). We focused our subsequent investigation on developing colonies exhibiting the most abundant Y-shape pattern.

By following the construction of a large number of colonies, we identified four characteristic morphological stages that occur in a defined temporal manner (Figure 2A; Movie S2). Stage I, Y-shape formation (0–4 hr); stage II, Y-shape elongation (4–5 hr), whereby the Y-shape morphology is rapidly expanded by further cell divisions, generating elongated chains that occupy a large area; stage III, central thickening (6–11 hr), in which numerous cell divisions take place at the center of the colony, while the Y arms start branching. These central divisions expand radially until the produced cells reach the tips of the Y arms. Stage IV, colony expansion (>11 hr), where the colony further expands radially to give rise to a full-sized colony. A similar developmental program was observed to be executed by the undomesticated *B. subtilis* strain 3610 (Figure S1D), which forms elaborate biofilm assemblies (Branda et al., 2001). Investigating the formation of colonies derived from the less abundant linear and multi-branched patterns revealed a similar series of stages, including initial chain elongation, central thickening, and expansion (Figure S1E). Collectively, the defined developmental stages monitored, indicate the existence of "construction rules" required for building up a colony.

Y-Arm Cells Guide Colony Development

To study the directionality of Y-arm extension, we employed laser irradiation to eradicate specific cells within the Y arm, and followed their position by the addition of the red fluorescent stain propidium iodide (PI), which preferentially penetrates dead cells. Initially, we irradiated cells located at mid-position within single- or double-chained Y arm. In both cases, the irradiated arms extended normally, but the change in position of the labeled cells indicated that the Y arm extends in an asymmetric fashion, with cells located at the tip of the arm mainly contributing to this directed extension (Figures 2B and S2A). In accord, damaging cells close to the tip of a Y arm severely impaired arm extension compared to the non-irradiated arms (Figures 2C and S2B). Furthermore, irradiation of the leading cells located at the

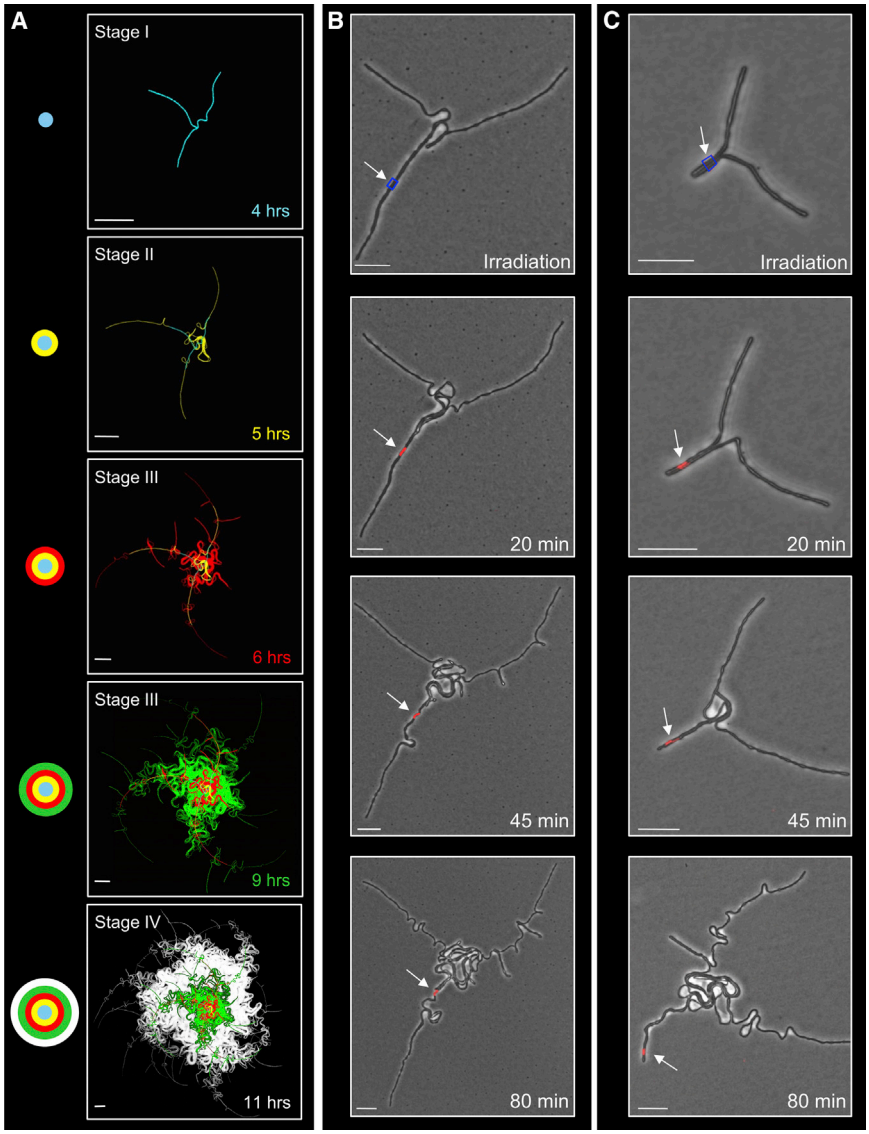

Figure 2. Characterizing Stages of Colony Development

(A) Time-lapse fluorescence images of AR16 (P_{rrnE}-*gfp*) developing colony at the defined stages and the indicated time points. Each stage was pseudo-colored and overlaid over previous stages. Color map corresponds to the different stages. Scale bars represent 40 μm.

(B and C) Cells (PY79) forming a Y shape were irradiated at the indicated position of the double-chained Y arm (blue frame). The irradiated cells were marked by the addition of PI (red), and their location (highlighted by arrows) was tracked at the indicated time points. Shown are overlaid transmitted light and fluorescence images. Representative experiments out of 13 independent biological repeats. Scale bars represent 20 μm.

tips of all three Y arms (Figure 3A; t = 4 hr) inflicted dramatic long-term consequences. Consistent with previous results, the reach of the Y arms was significantly reduced. At 2 hr post-irradiation (Figure 3A; t = 6 hr), the average length of the Y arms was 46 μm, while the Y arms of a similar non-irradiated colony reached an average of 136 μm. Moreover, hours later, the irradiated Y arms yielded a colony with a small diameter, occupying an area four times less than the non-irradiated colony (0.85 mm^2 compared to 3.29 mm^2) (Figure 3A; t = 8 hr). The size of the irradiated colony appeared to be constrained by the limited extension of the Y arms (Figure 3B). Remarkably, when an entire single Y arm was irradiated, the colony expanded in an asymmetric manner, failing to spread toward the area of the damaged Y arm (Figure 3C; Movie S3). These results emphasize the critical role of cells located at the arm's tip for arm elongation and indicate that the Y arm cells are guiding cells, as their reach determines the size and the architecture of the future colony.

YmdB Plays a Key Role in Directing the Early Stages of Colony Development

To gain insight into the genetic basis of the initial events of colony construction, an assortment of strains, harboring mutations in genes known to be involved in colony structure, biofilm formation, or motility, were screened for defects in Y-shaped formation (Table S1). A mutant in *ymdB*, encoding a phosphodiesterase previously implicated in biofilm formation (Diethmaier et al., 2011), was severely deficient in producing the characteristic Y shape or the linear and multi-branched structures. Instead, morphologies, missing noticeable extending arms or any other obvious pattern, were formed (Figure 4A). The average radial area occupied by colony founders of the *ΔymdB* strain, at a time parallel to Y-shaped formation, was calculated to be 6,000 ± 1,950 μm^2. At the same time, the average area captured by the same number of wild-type cells, forming the typical Y shape, was 15,100 ± 2,800 μm^2. Consistently, even after 20 hr of incubation, *ΔymdB* strain formed significantly smaller colonies than wild-type (Figure 4$D_{1 \text{ and } 2}$). In line with this view, cells, harboring *ymdB* under an inducible promoter as the sole *ymdB* copy, produced aberrant morphologies at a time equivalent to Y-shape formation, when grown in the absence of the inducer (Figure 4B; t = 3 hr). Supplementing the inducer at this stage could no longer restore the typical Y arms but resulted in resumption of cell chain extension projected at multiple directions (Figure 4B). Furthermore, the induced cells generated a considerably larger colonies containing a higher number of progeny in comparison to the non-induced ones, suggesting that the formation of extending arms could overcome the lack of Y shape (Figures 4B and 4C). Thus, YmdB plays a key role in directing early stages of colony development.

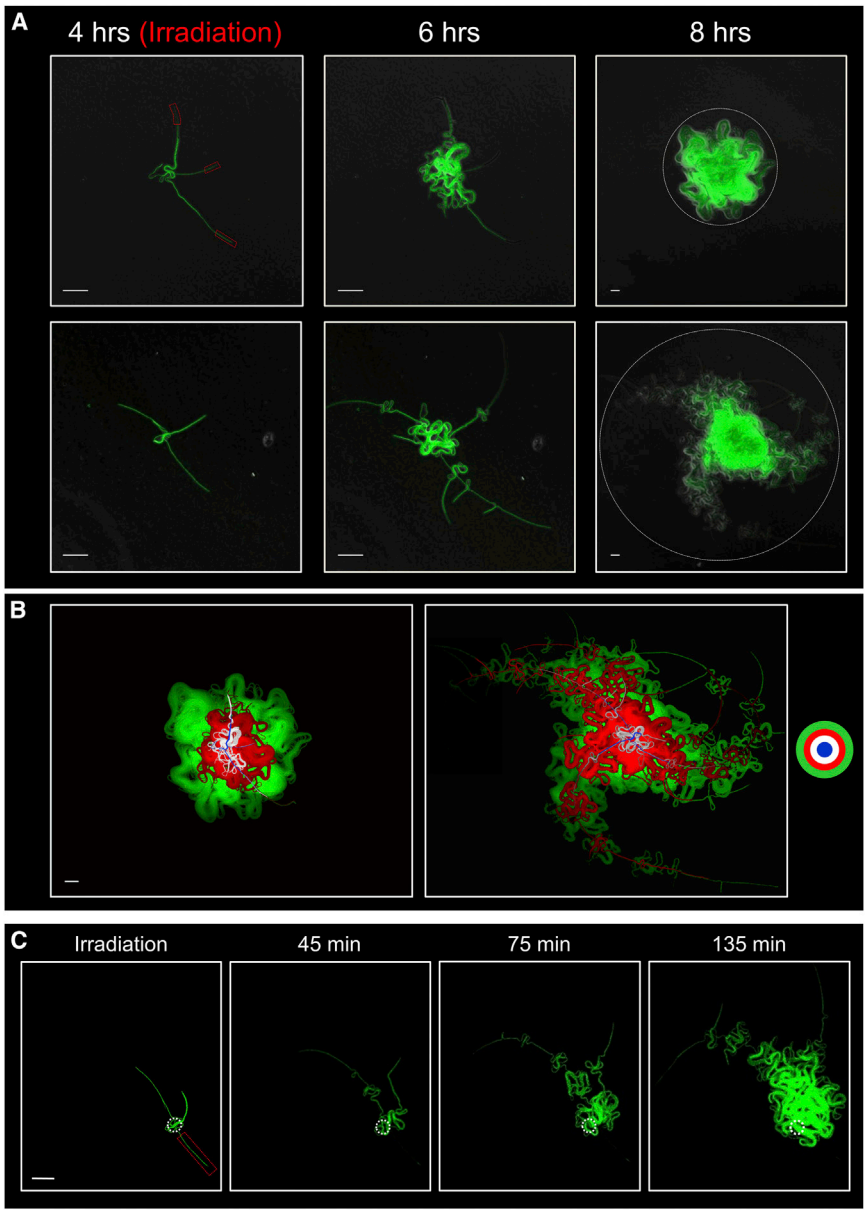

Figure 3. Early Stages of Colony Formation Determine Colony Morphology

(A) Fluorescence images overlaid with transmitted light images of AR16 (P_{rrnE}-*gfp*) cells at the indicated time points during colony formation. Top: the leading cells of a developing colony at t = 4 hr were irradiated (red boxes). Bottom: an untreated colony followed in parallel, as a control. Circle marks the radial area occupied by a developing colony. Representative experiment out of four independent biological repeats.

(B) Different stages of the developing colonies in (A) were pseudo-colored and overlaid. Shown are irradiated (left) and non-irradiated (right) colonies. Color map corresponds to the different stages, with the blue circle representing the earliest time point. Note the blue and the white layers of Y-shape stages that mark the reach of the irradiated colony (left).

(C) An entire Y arm of a developing AR16 colony was irradiated (red box) and colony formation followed at the indicated time points by CLSM. White circle represents the position of the progenitor cell. Representative experiment out of 12 independent biological repeats. Scale bars represent 40 μm.

Intracellular cAMP Levels Correlate with Colony Shape

YmdB is a phosphodiesterase that hydrolyzes cyclic nucleotides, such as cyclic AMP (cAMP) (Shin et al., 2008). So far, cAMP has been detected in *B. subtilis* cells only under anaerobic conditions (Mach et al., 1984). Using highly sensitive ELISA assay, we were able to detect low levels of cAMP in extracts from wild-type growing cells (Figure 4D_4). Furthermore, measuring the intracellular cAMP levels showed a large increase in YmdB mutant in comparison to wild-type (Figure 4D_4). To investigate if YmdB catalytic activity is required for Y-shape formation, we mutated the YmdB catalytic site (YmdB-D8A) (Diethmaier et al., 2014). Accordingly, cAMP levels within this strain were increased (Figure 4D_4). The mutant strain largely displayed aberrant colony morphologies at the time corresponding to Y-shape formation (Figures 4D_3 and S3A) and generated a small colony after 20 hr (Figure 4$D_{1\ and\ 2}$). Thus, intracellular cAMP level likely affects the ability to form a Y shape and eventually to produce a full-sized colony. We next tested whether adenylate cyclase (AC), which is known to synthesize cAMP (Danchin, 1993; Gancedo, 2013), influences colony development. Searching the *B. subtilis* genome for a potential AC did not yield an obvious candidate; nevertheless, an uncharacterized protein, YjbK, was found to harbor a potential AC catalytic site (Iyer and Aravind, 2002) (Figure S3B). Deletion of *yjbK* had no significant effect on colony size, Y-shape formation, or cAMP levels (Figures S3C–S3F). Furthermore, introducing Δ*yjbK* mutation into the *ΔymdB* strain did not restore colony size (Figures S3C and S3D). However, we found that YmdB levels corresponded to YjbK production, as overexpression of YjbK was associated with increased level of YmdB (Figure S3G), suggesting that the expression of these two proteins, potentially having opposing activities, is coordinated.

Evidence that Intercellular Nanotubes Contribute to Colony Formation

We have recently found that YmdB is required for efficient formation of intercellular nanotubes that bridge neighboring cells to allow molecular exchange (Dubey and Ben-Yehuda, 2011; Dubey et al., 2016; Pande et al., 2015). To investigate if such communication might be involved in colony establishment,

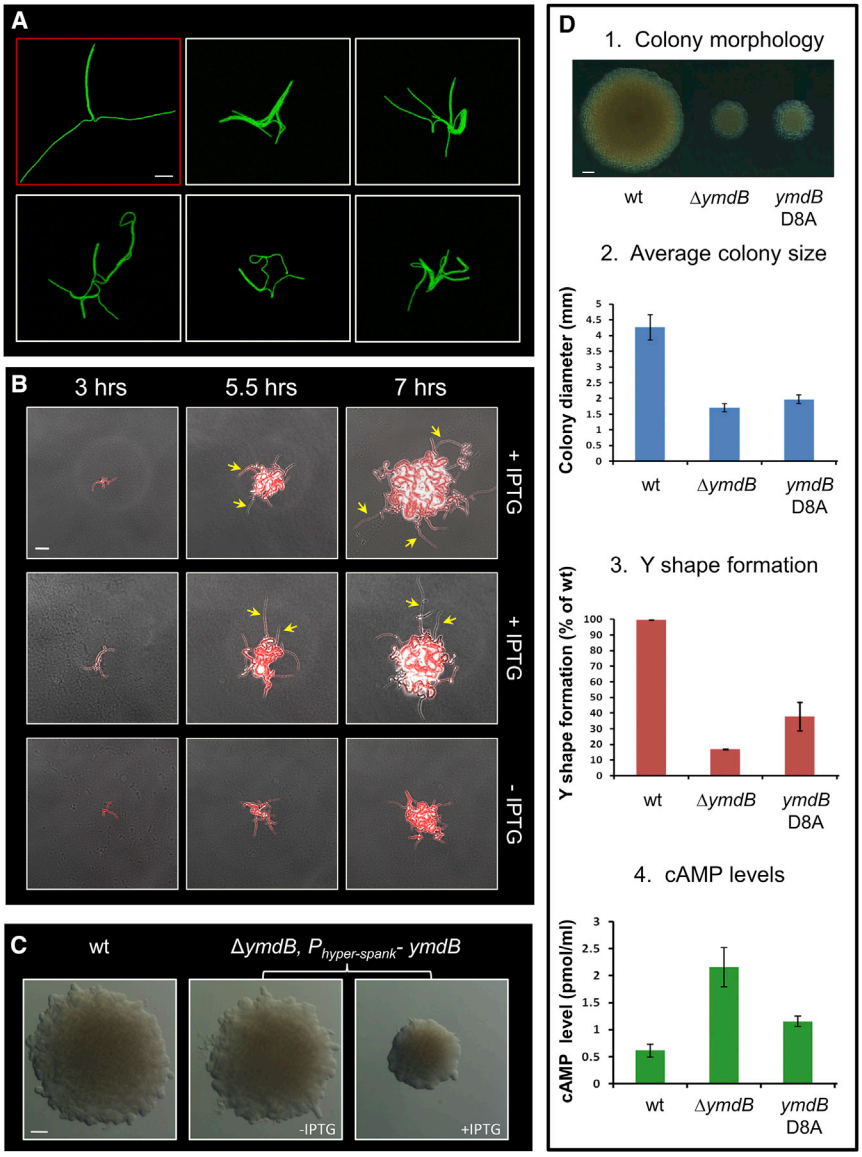

Figure 4. *ymdB* Mediates Proper Colony Establishment

(A) Fluorescence images of wild-type (AR16) and *ΔymdB* (GB112) cells expressing P_{rrnE}-*gfp*. Shown are images of a typical wild-type colony residing at stage I (top left, red frame; t = 3.5 hr) and five independent *ΔymdB* colonies at the equivalent stage of colony development (white frames; t = 3.5–4 hr). Scale bar, 10 μm.

(B) Fluorescence images (red) overlaid with transmitted light images (gray) of GB118 (*ΔymdB,* $P_{hyper\text{-}spank}$-*ymdB, rpsB*-mCherry) cells. Developing colonies were initiated in the absence of isopropyl β-D-1-thiogalactopyranoside (IPTG), and at t = 3 hr, IPTG was added. Examples of two different colonies at the indicated time points (top and middle) (+IPTG). In parallel, cells were grown without IPTG throughout the experiment (bottom) (−IPTG). Arrows indicate cell chains projected at multiple directions. Scale bar, 40 μm.

(C) PY79 (wild-type) and GB115 (*ΔymdB,* $P_{hyper\text{-}spank}$-*ymdB*) strains were grown on LB solid medium and incubated at 37°C for 20 hr. Strain GB115 was grown with or without IPTG as indicated. Shown are typical colonies photographed using a binocular. Scale bar, 0.5 mm.

(D) (1) The indicated strains were grown on LB solid medium and incubated at 37°C for 20 hr. Shown are typical colonies photographed using a binocular. Scale bar, 0.5 mm. (2) Average diameter of ~100 colonies of each indicated strain grown as described in (D_1). (3) Percentage of initial colony morphologies exhibiting a normal Y shape in comparison to wild-type (100%). For each strain, at least 100 developing colonies were examined. (4) Intracellular cAMP level of 1 ml cells (optical density 600 [OD_{600}] 0.7 ~5 × 10^8 cells/ml) of the indicated strains grown in liquid medium as measured by ELISA assay. Error bars represent three biological repeats (see Supplemental Experimental Procedures).

Y-shaped developing colonies were examined for the presence of nanotubes. Cells were followed utilizing CLSM and then imaged using high-resolution scanning electron microscopy (HR-SEM). This analysis revealed the existence of extensive intercellular tubular networks emanating from bacteria and occupying the space between the Y arms (Figure 5A), similar in appearance to the nanotube webs we observed at low cell density (Dubey et al., 2016). Yet, they were generally more challenging to detect, since they appeared to be partially buried within the relatively soft agarose surface. Importantly, these structures were clearly less abundant in the aberrant developing colonies produced by the *ΔymdB* mutant (Figures 5B and S4A). To examine the potential impact of the extracellular structures on colony formation, we attempted to damage them by particularly irradiating the area surrounding the cells. Correlative CLSM-HR-SEM analysis confirmed that treated areas were depleted from the nanotubular structures in comparison to non-treated proximal regions, while the cells appeared intact (Figures S4B, S4C, and S5A). Notably, we cannot exclude the possibility that other extracellular structures were damaged by this procedure. Nevertheless, when we precisely irradiated the intercellular area between the Y arms, we observed a significant developmental delay followed by an atypical colony morphology. Such treatment had little effect on Y-arm extension; however, the majority of the newly dividing cells branched from the Y arms instead of displaying the characteristic thickening at the center (Figures 5C and 5D). As a control, we irradiated intercellular regions slightly away from the extending Y arms; however, such treatment did not significantly affect colony development (Figure S5B). Additionally, fluorescence recovery after photobleaching experiments of small molecules within the agar revealed the recovery time to be very short (≤1.5 min), implying that if any toxic molecules were formed due to the treatment they were likely to diffuse rapidly (Figure S5C). We have previously

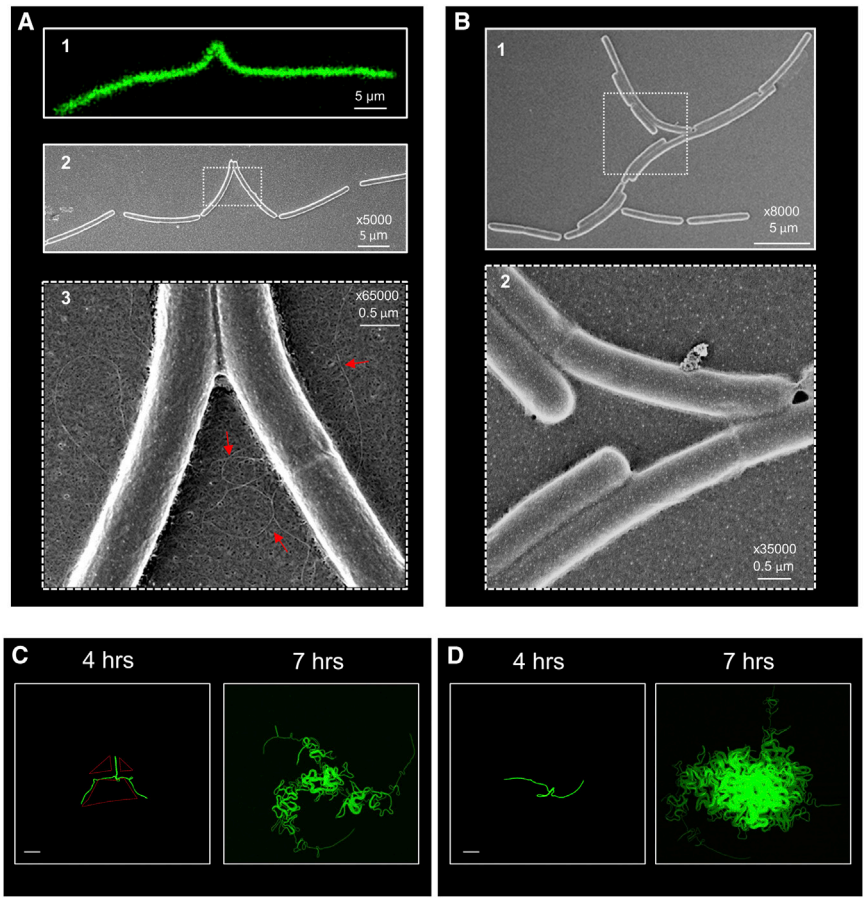

Figure 5. Evidence that Intercellular Nanotubes Contribute to Colony Development

(A) AR16 (P_{rmE}-*gfp*) cells were followed by CLSM. At t = 3 hr, the cells were fixed, washed, gold coated, and observed with HR-SEM: (1) Fluorescence image of stage I colony. (2) HR-SEM image of the same colony at low magnification. Notably, cell position was slightly shifted during fixation. (3) Magnification of the boxed region in 2. Red arrows highlight intercellular tubular structures.

(B) GB61 (*ΔymdB*) cells were treated as in (A). (1) Low-magnification HR-SEM image. (2) Magnification of the boxed region in 1.

(C and D) Time-lapse fluorescence images of AR16 developing colonies.

(C) The intercellular region between the three Y arms (t = 4 hr) was irradiated, and colony was photographed at t = 7 hr.

(D) Untreated colony was followed in parallel. Scale bars represent 20 μm.

shown that the presence of SDS perturbs nanotube formation (Dubey and Ben-Yehuda, 2011). Consistently, colony development on SDS containing agar resulted in the production of aberrant patterns of developing colonies (Figure S5D; Movie S4). Taken together, these results support the view that nanotubes contribute to colony formation by facilitating communication among colony founders.

DISCUSSION

Based on our analysis, we propose the following model for colony establishment in *B. subtilis*. A single progenitor cell undergoes initial divisions creating a chain of progeny cells, which tends to break early on to produce arms, typically extending in a Y-shaped structure. The cells located at the tips of the Y arms propagate away from the colony center to define the borders of the future colony, marking a large radial area in clock needle-like fashion. Nanotube networks formed among the Y arms facilitate their coordination to enable the subsequent stage of central thickening. During this phase, the cells divide extensively mainly at the colony center until reaching the borders marked by the leader cells. Success or failure to properly perform these primary stages has a deterministic impact on the size and morphology of the future colony and, most importantly, on the efficiency of progeny production. Intriguingly, we found that similar to *B. subtilis, Bacillus cereus* occupies a large territory prior to an extensive division phase that fills up the entire marked area (Movie S5), suggesting that this approach is not restricted to *B. subtilis* and likely maximizes bacterial propagation in natural habitats.

The multi-directional growth of the leading cells early during development is most likely guided by cAMP levels, as a clear correlation was observed between Y-shape formation, intracellular cAMP levels, and the final colony size (Figure 4D). YmdB acts to control the internal cAMP level, which in turn determines colony fate. Other phosphodiesterases and opposing ACs, such as YjbK, could be additional determinants, affecting the overall cellular cAMP levels. It still remains to be explored how cAMP levels modulate colony growth; however, the finding that the mRNA levels of >800 genes change in the absence of YmdB (Diethmaier et al., 2014) suggests large amount of cAMP-responsive proteins. In light of this view, cAMP is a key molecule in chemotaxis, motility, and multicellular assemblies in several microorganisms, such as *Dictyostelium*, *Trypanosoma*, *Vibrio*, and *Pseudomonas* (Firtel and Meili, 2000; Huynh et al., 2012; Liang et al., 2007; Lopez et al., 2015). Furthermore, cAMP was found to induce switching in turning direction of nerve growth cones (Song et al., 1997), highlighting its importance in guiding cell growth directionality in nature.

EXPERIMENTAL PROCEDURES

Bacterial Strains and Plasmids

Bacterial strains used in this study are listed in Table S2, plasmid constructions are described in Table S3, and primers are listed in Table S4.

Live Imaging of Developing Colonies

A custom-designed construct was used to grow bacterial colonies under the microscope. A 40-mm metal ring was filled with LB agarose (1.5%)

and assembled as described in Figures S1A and S1B. Bacterial cells were spotted at a concentration of one cell per microliter. When indicated, cells were stained by adding FM1-43, FM4-64 (Invitrogen) fluorescent membrane dyes, or propidium iodide (PI) (Sigma) to the solid LB medium at a final concentration of 1 μg/ml (FM1-43, FM4-64) and 5 μg/ml (PI). Colony growth construct was covered with a 35-mm cultFoil membrane (Pecon) to reduce agar dehydration and incubated in Lab-Tek S1 heating insert (Pecon) placed inside an incubator XL-LSM 710 S1 (Pecon). Developing colonies were visualized and photographed by CLSM LSM700 (Zeiss) with Plan-Apochromat ×10/NA0.45 or LD-Plan Neufloar ×20/NA0.4 lenses (Zeiss), and single cells were photographed with a Plan-Apochromat ×100/NA1.4 lens (Zeiss). Cells expressing GFP or stained with FM1-43 were irradiated using 488-nm laser beam, while cells expressing mCherry or stained with FM4-64 or PI were irradiated using a 555-nm laser beam. For each experiment, both transmitted and reflected light were collected. For intervening with colony development by irradiating specific cells or cell surrounding areas, regions were defined and marked as regions for bleaching. Bleaching was performed using the 405-nm laser beam at full power (5 mW) and the regions were repeatedly bleached, 25–50 iterations. Similar conditions were used when the sample was further analyzed by HR-SEM for correlative microscopy (see below). System control and image processing were carried out using Zen software version 8.0 (Zeiss). In order to create overlay images of stages of colony development, each stage was pseusocolored differentially and the images were overlaid as separate layers with the earliest time point on top.

Correlative CLSM-HR-SEM Procedure

For sample preparations, LB agarose (3%) was poured onto a 25 mm round cover glass and gently pressed with a slide to form a uniform thin layer of solid medium. Exponentially growing *B. subtilis* cells were diluted, spread on the agarose surface and incubated under the microscope until early stages of colony development were visible (2-4 hr). Next, cells were fixed with 2% glutaraldehyde in 0.1 M sodium cacodylate buffer ($Na\ (CH_3)_2\ AsO_2 \cdot 3H_2O$ [pH 7.2]) for 2 hr at 25°C and then washed three times with 0.1 M sodium cacodylate buffer. Specimens were coated with gold-palladium (~8 nm cluster size) with Quorum Technologies SC7640 Sputter Coater, and cells were observed with a FEG EHR-SEM (Magellan 400L [FEI]).

Additional procedures including general methods, measuring the radial area occupied by a developing colony, testing diffusion rates of small molecules on agarose pads, and cAMP ELISA testing are described in the Supplemental Experimental Procedures.

SUPPLEMENTAL INFORMATION

Supplemental Information includes Supplemental Experimental Procedures, five figures, four tables, and five movies and can be found with this article online at http://dx.doi.org/10.1016/j.celrep.2016.01.071.

AUTHOR CONTRIBUTIONS

Conceptualization, G.M., G.B.M.M., A. Rouvinski, and S.B.-Y.; Methodology, G.M., A. Rouvinski, and S.B.-Y.; Investigation, G.M., G.B.M.M., and S.B.-Y.; Writing – Original Draft, G.M and S.B.-Y.; Writing –Review & Editing, G.M., G.B.M.M., A. Rouvinski, A. Rosenberg, and S.B.-Y; Funding Acquisition, S.B.-Y; Resources, A. Rosenberg.

ACKNOWLEDGMENTS

We thank E. Blayvas (Hebrew University) for support during EM analysis the and National BioResource Project National Institute of Genetics, Japan for *B. subtilis* mutant strains. We are grateful to members of the S.B.-Y. laboratory and G. Bachrach, I. Rosenshine, and A. Taraboulos (Hebrew University) for valuable comments. This work was supported by a European Research Council Advance Grant (339984) and by the Israel Science Foundation (327/11) awarded to S.B.-Y. G.B.M.M. was supported by the Israeli Council for Higher Education PBC-outstanding postdoctoral fellowship.

Received: October 7, 2015
Revised: November 30, 2015
Accepted: January 22, 2016
Published: February 18, 2016

REFERENCES

Be'er, A., Zhang, H.P., Florin, E.L., Payne, S.M., Ben-Jacob, E., and Swinney, H.L. (2009). Deadly competition between sibling bacterial colonies. Proc. Natl. Acad. Sci. USA *106*, 428–433.

Ben-Jacob, E., and Levine, H. (2006). Self-engineering capabilities of bacteria. J. R. Soc. Interface *3*, 197–214.

Branda, S.S., González-Pastor, J.E., Ben-Yehuda, S., Losick, R., and Kolter, R. (2001). Fruiting body formation by *Bacillus subtilis*. Proc. Natl. Acad. Sci. USA *98*, 11621–11626.

Branda, S.S., González-Pastor, J.E., Dervyn, E., Ehrlich, S.D., Losick, R., and Kolter, R. (2004). Genes involved in formation of structured multicellular communities by *Bacillus subtilis*. J. Bacteriol. *186*, 3970–3979.

Branda, S.S., Vik, S., Friedman, L., and Kolter, R. (2005). Biofilms: the matrix revisited. Trends Microbiol. *13*, 20–26.

Branda, S.S., Chu, F., Kearns, D.B., Losick, R., and Kolter, R. (2006). A major protein component of the *Bacillus subtilis* biofilm matrix. Mol. Microbiol. *59*, 1229–1238.

Christensen, B.B., Haagensen, J.A., Heydorn, A., and Molin, S. (2002). Metabolic commensalism and competition in a two-species microbial consortium. Appl. Environ. Microbiol. *68*, 2495–2502.

Danchin, A. (1993). Phylogeny of adenylyl cyclases. Adv. Second Messenger Phosphoprotein Res. *27*, 109–162.

Diethmaier, C., Pietack, N., Gunka, K., Wrede, C., Lehnik-Habrink, M., Herzberg, C., Hübner, S., and Stülke, J. (2011). A novel factor controlling bistability in *Bacillus subtilis*: the YmdB protein affects flagellin expression and biofilm formation. J. Bacteriol. *193*, 5997–6007.

Diethmaier, C., Newman, J.A., Kovács, A.T., Kaever, V., Herzberg, C., Rodrigues, C., Boonstra, M., Kuipers, O.P., Lewis, R.J., and Stülke, J. (2014). The YmdB phosphodiesterase is a global regulator of late adaptive responses in *Bacillus subtilis*. J. Bacteriol. *196*, 265–275.

Dubey, G.P., and Ben-Yehuda, S. (2011). Intercellular nanotubes mediate bacterial communication. Cell *144*, 590–600.

Dubey, G.P., Malli Mohan, G.B., Dubrovsky, A., Amen, T., Tsipshtein, S., Rouvinski, A., Rosenberg, A., Kaganovich, D., Sherman, E., Medalia, O., and Ben-Yehuda, S. (2016). Architecture and Characteristics of Bacterial Nanotubes. Dev. Cell *36*, 453–461.

Firtel, R.A., and Meili, R. (2000). Dictyostelium: a model for regulated cell movement during morphogenesis. Curr. Opin. Genet. Dev. *10*, 421–427.

Flemming, H.C., Neu, T.R., and Wozniak, D.J. (2007). The EPS matrix: the "house of biofilm cells". J. Bacteriol. *189*, 7945–7947.

Gancedo, J.M. (2013). Biological roles of cAMP: variations on a theme in the different kingdoms of life. Biol. Rev. Camb. Philos. Soc. *88*, 645–668.

Huynh, T.T., McDougald, D., Klebensberger, J., Al Qarni, B., Barraud, N., Rice, S.A., Kjelleberg, S., and Schleheck, D. (2012). Glucose starvation-induced dispersal of *Pseudomonas aeruginosa* biofilms is cAMP and energy dependent. PLoS ONE *7*, e42874.

Iyer, L.M., and Aravind, L. (2002). The catalytic domains of thiamine triphosphatase and CyaB-like adenylyl cyclase define a novel superfamily of domains that bind organic phosphates. BMC Genomics *3*, 33.

Kaiser, D. (2006). A microbial genetic journey. Annu. Rev. Microbiol. *60*, 1–25.

Kaufmann, S.H.E., and Schaible, U.E. (2005). 100th anniversary of Robert Koch's Nobel Prize for the discovery of the tubercle *bacillus*. Trends Microbiol. *13*, 469–475.

Kearns, D.B., Chu, F., Branda, S.S., Kolter, R., and Losick, R. (2005). A master regulator for biofilm formation by *Bacillus subtilis*. Mol. Microbiol. *55*, 739–749.

Lewis, K. (2001). Riddle of biofilm resistance. Antimicrob. Agents Chemother. *45*, 999–1007.

Liang, W., Silva, A.J., and Benitez, J.A. (2007). The cyclic AMP receptor protein modulates colonial morphology in *Vibrio cholerae*. Appl. Environ. Microbiol. *73*, 7482–7487.

Lopez, M.A., Saada, E.A., and Hill, K.L. (2015). Insect stage-specific adenylate cyclases regulate social motility in African trypanosomes. Eukaryot. Cell *14*, 104–112.

Mach, H., Hecker, M., and Mach, F. (1984). Evidence for the presence of cyclic adenosine-monophosphate in *Bacillus subtilis*. FEMS Microbiol. Lett. *22*, 27–30.

Mauriello, E.M., and Zusman, D.R. (2007). Polarity of motility systems in *Myxococcus xanthus*. Curr. Opin. Microbiol. *10*, 624–629.

Moons, P., Michiels, C.W., and Aertsen, A. (2009). Bacterial interactions in biofilms. Crit. Rev. Microbiol. *35*, 157–168.

Pande, S., Shitut, S., Freund, L., Westermann, M., Bertels, F., Colesie, C., Bischofs, I.B., and Kost, C. (2015). Metabolic cross-feeding via intercellular nanotubes among bacteria. Nat. Commun. *6*, 6238.

Shin, D.H., Proudfoot, M., Lim, H.J., Choi, I.K., Yokota, H., Yakunin, A.F., Kim, R., and Kim, S.H. (2008). Structural and enzymatic characterization of DR1281: a calcineurin-like phosphoesterase from *Deinococcus radiodurans*. Proteins *70*, 1000–1009.

Song, H.J., Ming, G.L., and Poo, M.M. (1997). cAMP-induced switching in turning direction of nerve growth cones. Nature *388*, 275–279.

Zhang, Y., Ducret, A., Shaevitz, J., and Mignot, T. (2012). From individual cell motility to collective behaviors: insights from a prokaryote, *Myxococcus xanthus*. FEMS Microbiol. Rev. *36*, 149–164.

Cell Reports, Volume *14*

Supplemental Information

Early Developmental Program Shapes Colony Morphology in Bacteria

Gideon Mamou, Ganesh Babu Malli Mohan, Alex Rouvinski, Alex Rosenberg, and Sigal Ben-Yehuda

Figure S1

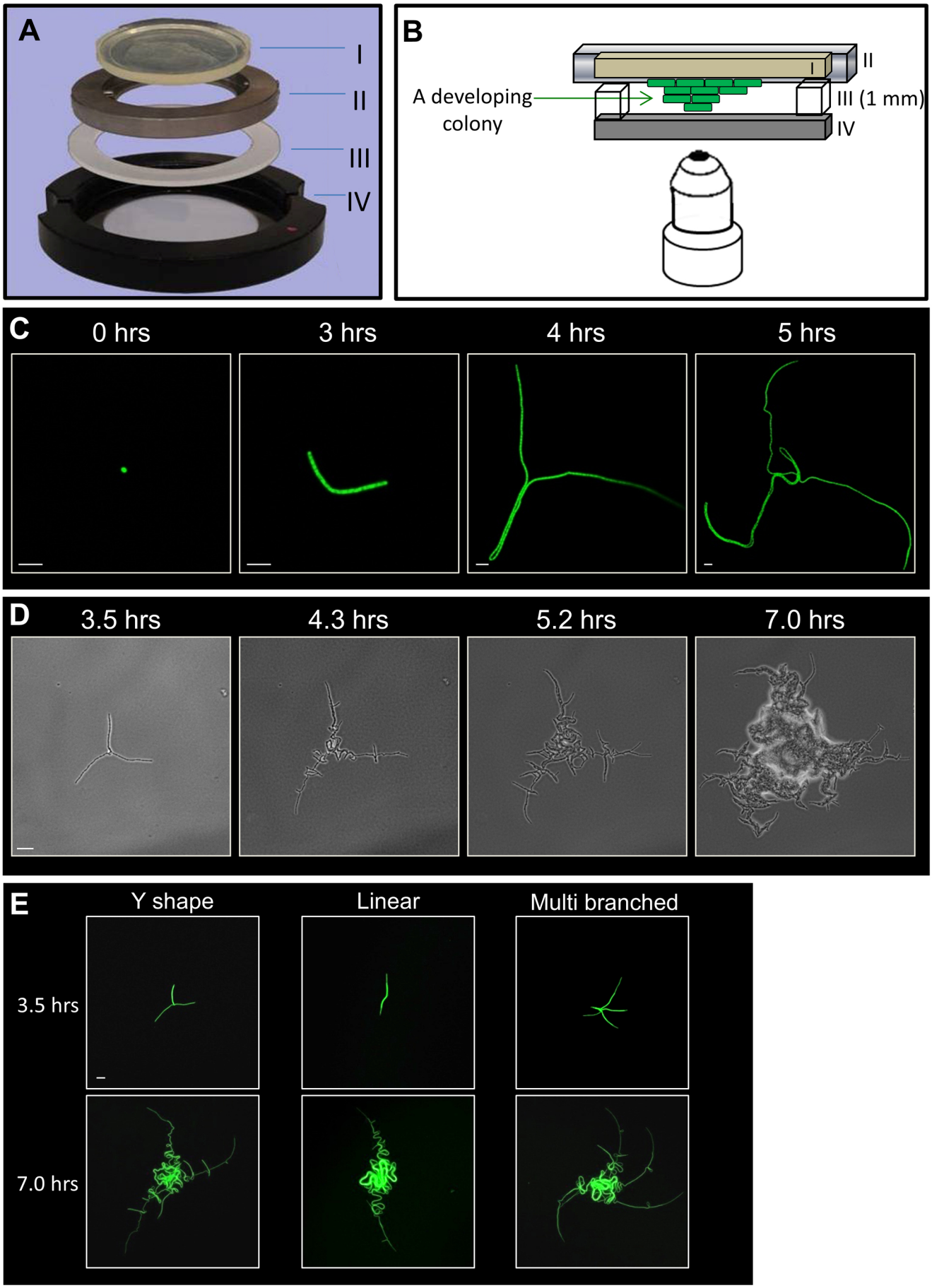
A
I
II
III
IV
B
A developing colony
II
III (1 mm)
IV
C
0 hrs
3 hrs
4 hrs
5 hrs
D
3.5 hrs
4.3 hrs
5.2 hrs
7.0 hrs
E
Y shape
Linear
Multi branched
3.5 hrs
7.0 hrs

Figure S2

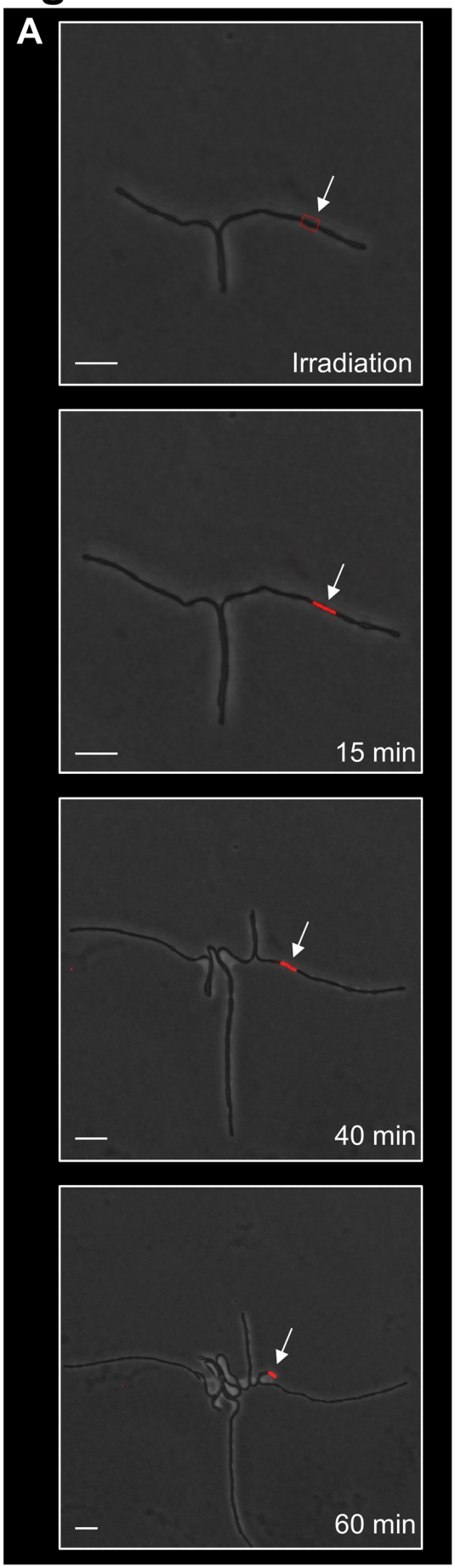
A
Irradiation
15 min
40 min
60 min

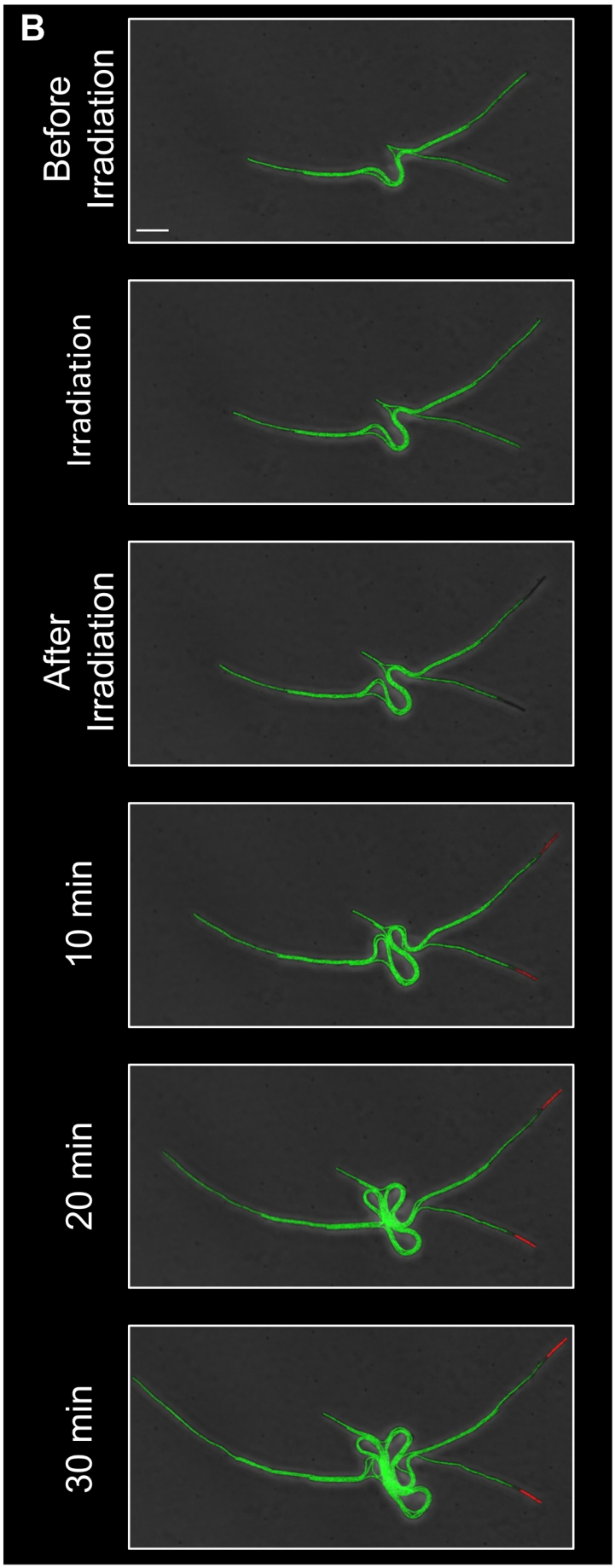
B
Before Irradiation
Irradiation
After Irradiation
10 min
20 min
30 min

Figure S3

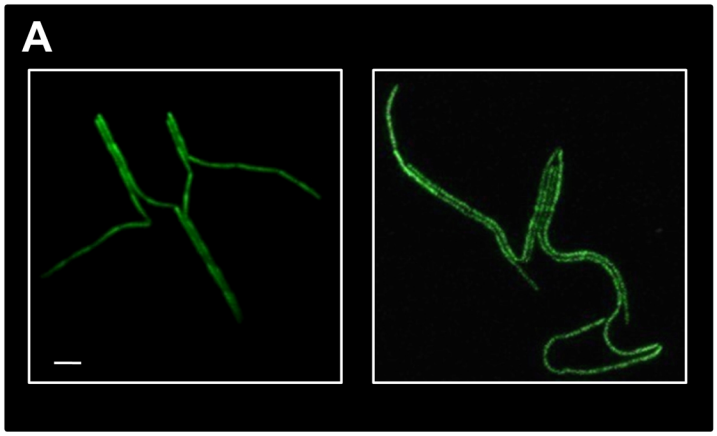
A

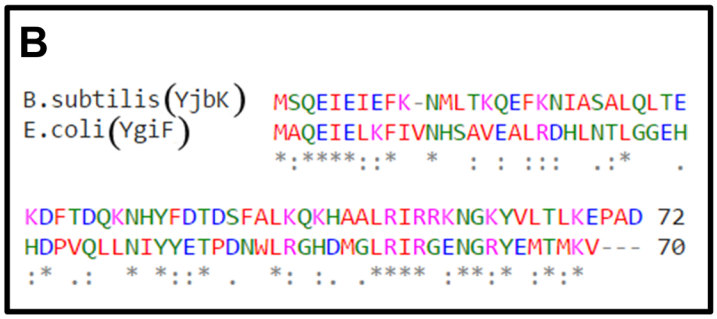
B
B.subtilis (YjbK) MSQEIEIEFK-NMLTKQEFKNIASALQLTE
E.coli (YgiF) MAQEIELKFIVNHSAVEALRDHLNTLGGEH
KDFTDQKNHYFDTDSFALKQKHAALRIRRKNGKYVLTLKEPAD 72
HDPVQLLNIYYETPDNWLRGHDMGLRIRGENGRYEMTMKV--- 70

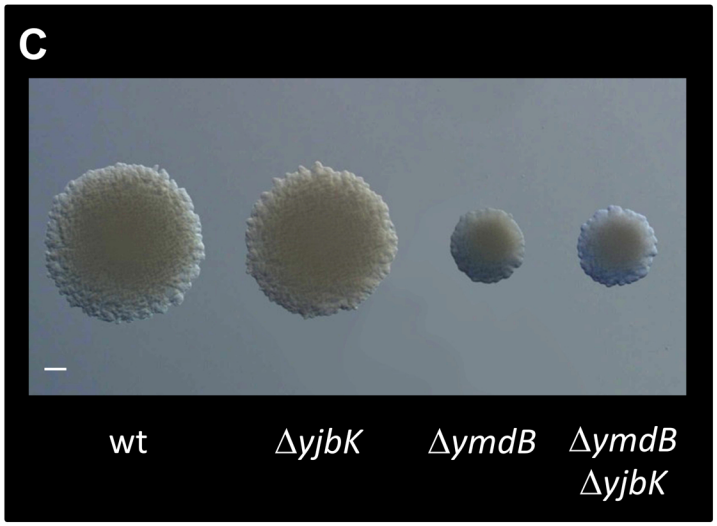
C
wt
ΔyjbK
ΔymdB
ΔymdB ΔyjbK

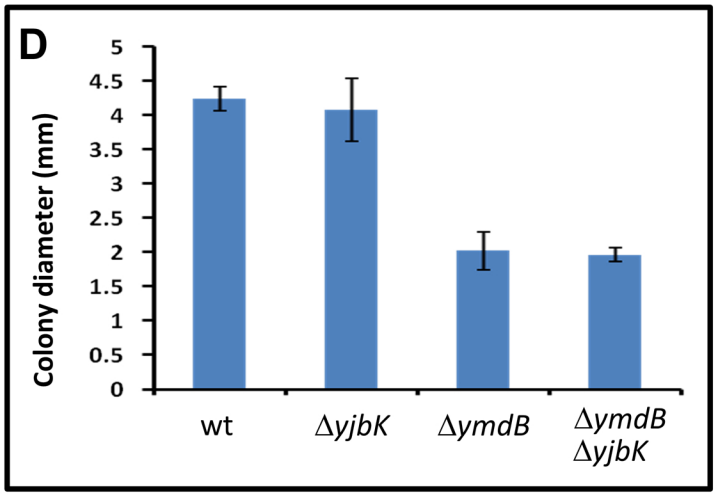
D
Colony diameter (mm)
0
0.5
1
1.5
2
2.5
3
3.5
4
4.5
5
wt
ΔyjbK
ΔymdB
ΔymdB ΔyjbK

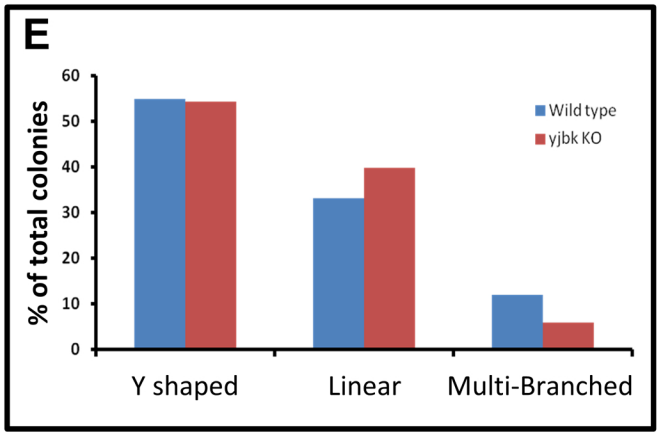
E
% of total colonies
0
10
20
30
40
50
60
Wild type
yjbk KO
Y shaped
Linear
Multi-Branched

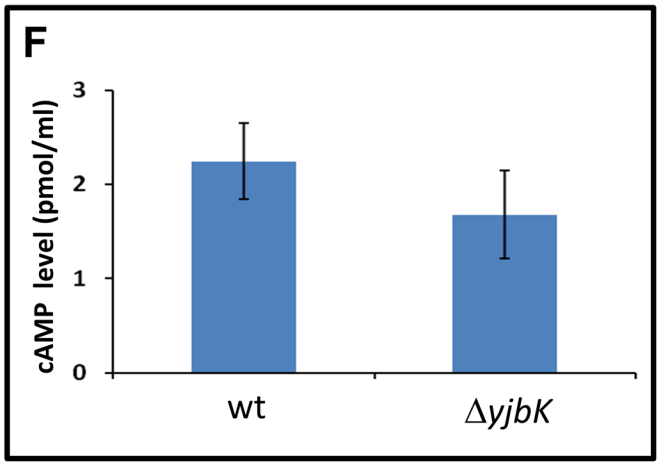
F
cAMP level (pmol/ml)
0
1
2
3
wt
ΔyjbK

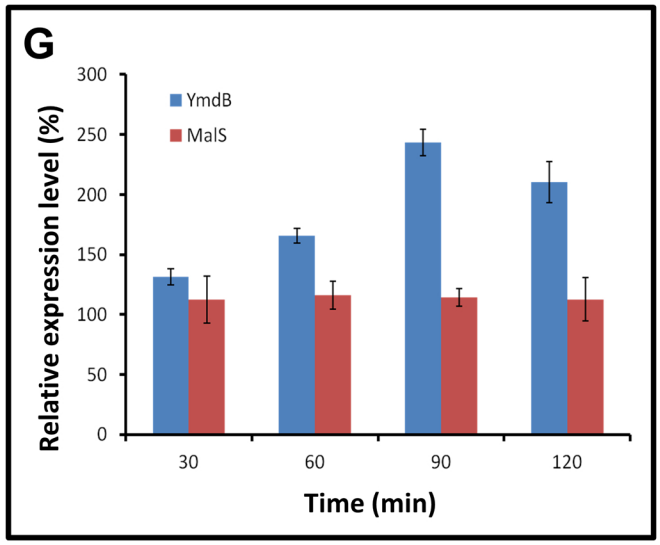
G
Relative expression level (%)
0
50
100
150
200
250
300
YmdB
MalS
30
60
90
120
Time (min)

Figure S4

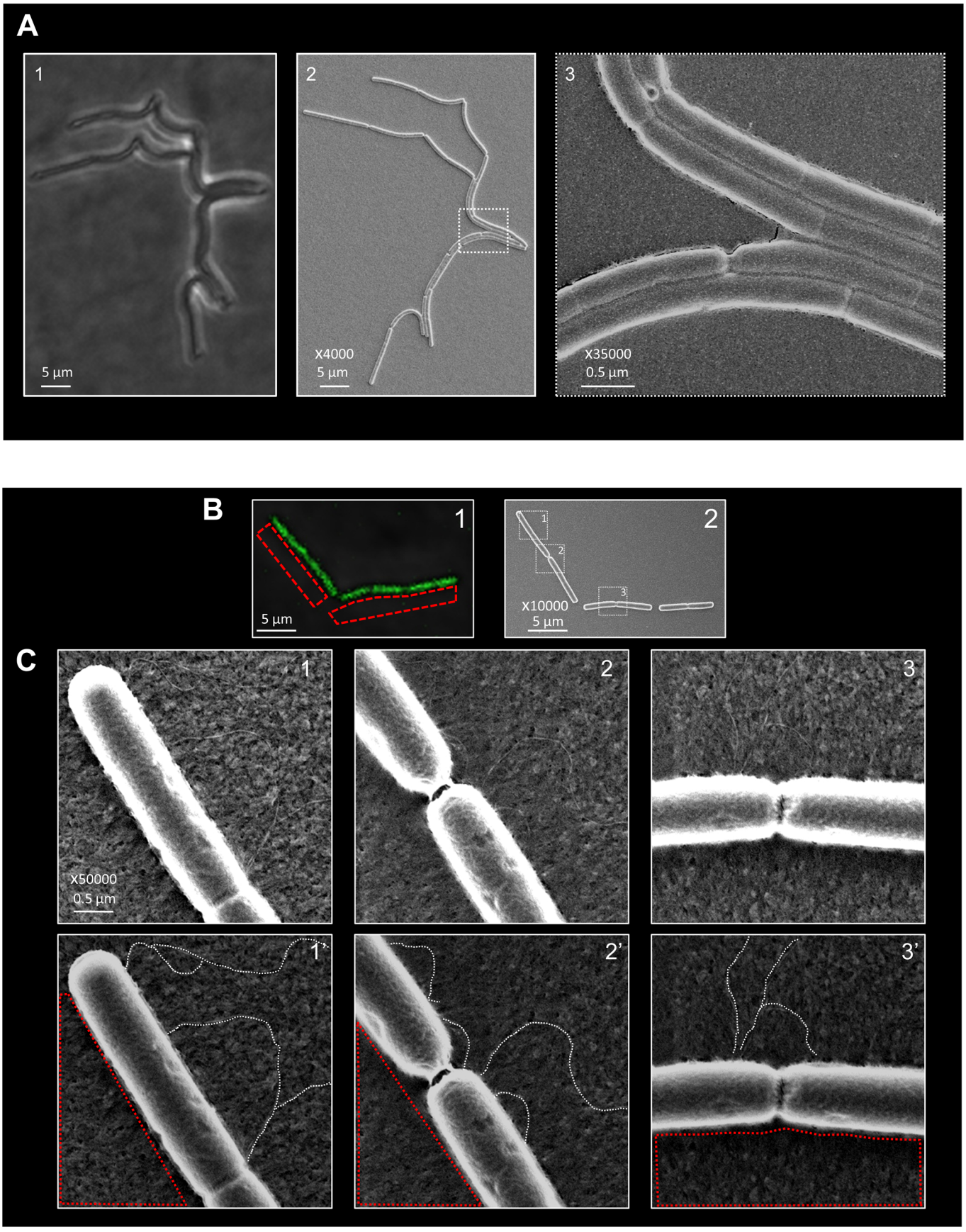
A
1
5 µm
2
X4000
5 µm
3
X35000
0.5 µm
B
1
5 µm
2
1
2
3
X10000
5 µm
C
1
X50000
0.5 µm
2
3
1'
2'
3'

Figure S5

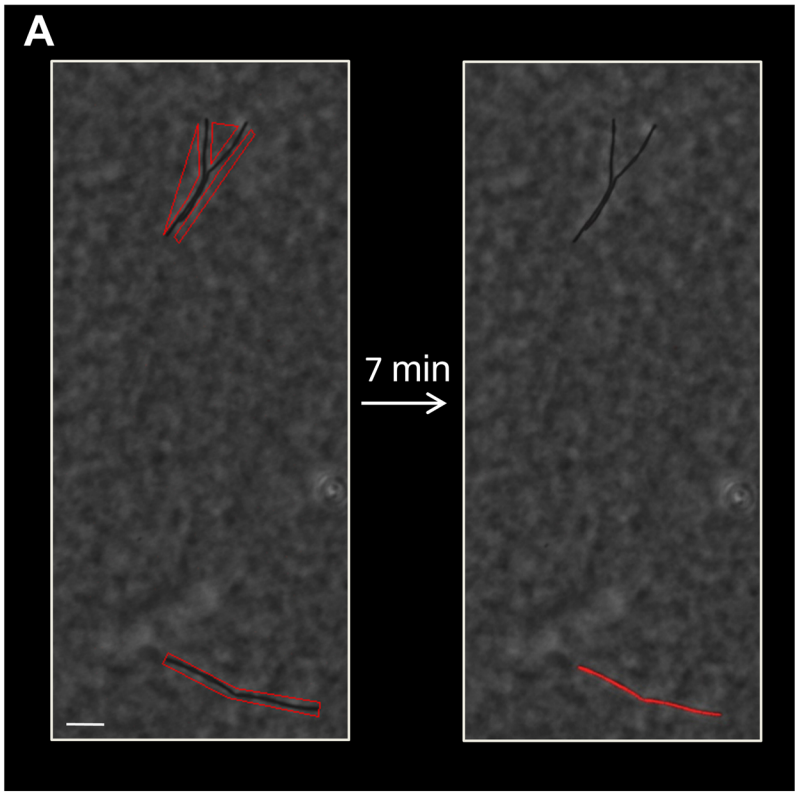
A
7 min

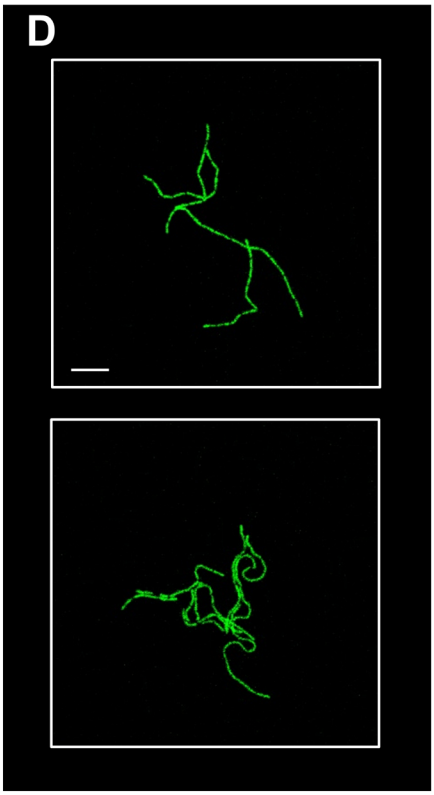
D

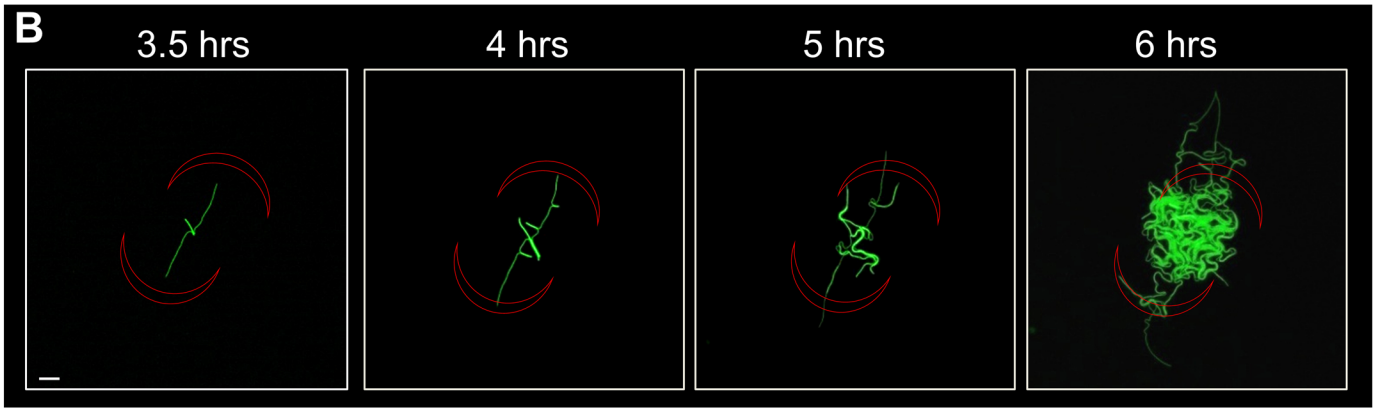
B
3.5 hrs
4 hrs
5 hrs
6 hrs

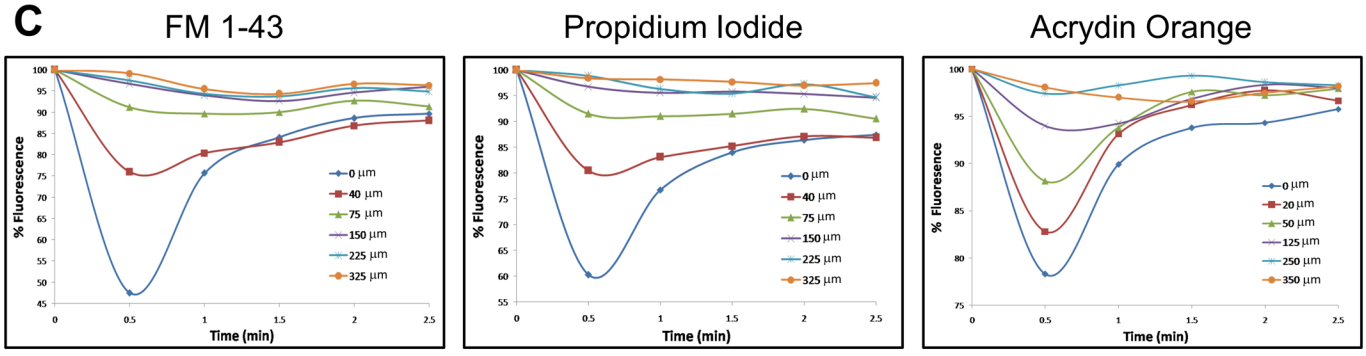
C
FM 1-43
Propidium Iodide
Acrydin Orange
% Fluorescence
Time (min)
0 µm
40 µm
75 µm
150 µm
225 µm
325 µm
20 µm
50 µm
125 µm
250 µm
350 µm

Table S1: List of genes examined in this study for the early stages of colony development

Strain name	Mutant gene(s)	Gene function	Observed effect on Y shape formation	Reference
GD215	Δ*hag*	Flagellum subunit	No effect	(Mirel and Chamberlin, 1989)
SG157	Δ*tasA*	Production of an ECM protein	No effect	(Branda et al., 2006; Serrano et al., 1999)
GD278	Δ*tasA*, Δ*hag*		No effect	
SB781	Δ*spo0A*	Master regulator of sporulation, affects biofilm formation.	Small effect, sometimes Y arms seem shorter	(Branda et al., 2001)
GD413	Δ*sinR*	Transcriptional regulator, repressor of many biofilm formation genes.	No effect	(Kearns et al., 2005)
GD420	Δ*sinI*	Antagonist of SinR	Small effect, sometimes Y arms seem shorter and curlier	(Kearns et al., 2005)
GM3	Δ*yvfA*	Antagonist of SinR	No effect	(Tortosa et al., 2000)
GM5	Δ*veg*	Antagonist of SinR	Small effect, sometimes Y arms seem shorter	(Lei et al., 2013)
GM9	Δ*ylbF*	Antagonist of SinR	No effect	(Branda et al., 2004)
GB61	Δ*ymdB*	Phosphodiesterase, affects biofilm formation	Major defect in Y shape formation	(Diethmaier et al., 2011)
GM7	Δ*ecsB*	ABC transporter, involved in multicellularity	No effect	(Branda et al., 2004)
GM8	Δ*yqeK*	Predicted hydrolase, involved in multicellularity	No effect	(Branda et al., 2004)
GM10	Δ*yhxB*	Alpha-phosphoglucomutase, involved in multicellularity	No effect	(Branda et al., 2004)

All the strains are derivatives of the wild type strain PY79
GB61 (Δ*ymdB*), having a profound effect, is highlighted in blue.

Table S2: List of bacterial strains used in this study

Strain Name	Genotype	Description
PY79	Wild type	(Youngman et al., 1984)
AR5	*rplA-gfp-spc*	(Rosenberg et al., 2012)
AR6	*rpsB-mCherry-kan*	Constructed by integrating pAR5 into PY79 (Segev et al., 2013).
AR16	*amyE::P_{rrnE}-gfp-spc*	(Rosenberg et al., 2012)
GB61	*Δymd B::tet*	Constructed using Gibson assembly kit (NEB, USA) utilizing primers *ymdB::tet*-P1-P4.
GB112	*Δymd B::tet, amyE::P_{rrnE}-gfp-spc*	Constructed by transforming AR16 gDNA into GB61.
GB113	*ymdB-gfp-spc*	Constructed by integrating pGB10 into PY79.
GB115	*Δymd B::tet, amyE::$P_{hyper\text{-}spank}$- ymdB-spc*	Constructed by transforming linearized pGB11 into GB61.
GB118	*Δymd B::tet, amyE::$P_{hyper\text{-}spank}$-ymdB-spc, rpsB-mCherry-kan*	Constructed by transforming AR6 gDNA into GB115.
GB125	*ymdB D8A*	PY79 was transformed with pGB16. Next, transformants were patched and screened for mls sensitivity, indicating that the plasmid was popped out. The presence of the mutation was confirmed by PCR followed by DNA sequencing.
GB142	*ΔyjbK::spc*	Constructed using Gibson assembly kit (NEB, USA) utilizing primers *yjbK::spc*-P1-P4.
GB154	*amyE::$P_{hyper\text{-}spank}$-yjbK-spc*	Constructed by transforming pGB37 into PY79.
GB156	*ΔyjbK::spc, Δymd B::tet*	Constructed by transforming GB61 gDNA into GB142.
GB201	*ymdB D8A-gfp-spc*	Constructed by transforming pGB10 into GB125.
GB222	*amyE::$P_{hyper\text{-}spank}$-yjbK-spc, ymdB-gfp -kan*	Constructed by transforming pGB13 into GB154.
GD215	*hag*::*erm*	Constructed using Gibson assembly kit (NEB, USA) utilizing primers

		hag::erm-P1-P4.
GD278	*tasA::spec, hag::erm*	Constructed by transforming GD215 gDNA into SG157.
GD413	*sinR:spec*	Constructed using PCR based KO using primers *sinR::spec*-P1-P4.
GD420	*sinI:spec*	Constructed by transforming DS79 gDNA (a gift from D. Kearns, Indiana U) into PY79.
GM3	*yvfA:: pMUTIN -spec*	Genomic DNA from MGNA-B610 (*B. subtilis* Functional Analysis mutant collection) was inserted into PY79.
GM5	*Veg:: pMUTIN-spec*	Genomic DNA from MGNA-B909 (*B. subtilis* Functional Analysis mutant collection) was inserted into PY79.
GM7	*ΔecsB::spec*	Constructed using Gibson assembly kit (NEB, USA) utilizing primers *ecsB-ko* -P1-P4.
GM8	Δ*yqeK::kan*	Constructed using Gibson assembly kit (NEB, USA) utilizing primers Δ*yqeK-ko*-P1-P4.
GM9	Δ*ylbF::tet*	Constructed using Gibson assembly kit (NEB, USA) utilizing primers *ylbF-ko*-P1-P4
GM10	Δ*yhxB::kan*	Constructed using Gibson assembly kit (NEB, USA) utilizing primers *yhxB-ko*-P1-P4.
GM13	*ΔyjbK, amyE::*$P_{hyper\text{-}spank}$*- yjbK-spc, malS- gfp -kan*	Genomic DNA from LS75 was inserted into GB154 strain
LS75	*malS- gfp -kan*	Constructed by integrating pLS75 into PY79.
SB781	*spoA::erm*	Constructed by transforming PY79 with SIK31(Ireton et al., 1993).
SG157	*tasA::spec*	Constructed by transforming gDNA from strain bDR2181 (a gift from David Rudner, Harvard U) into PY79.
NCIB 3610	Undomesticated *B. subtilis* strain	(Branda et al., 2001)
Bacillus cereus	Natural isolate, 16S rDNA sequencing defined it as TA32-5 strain	*B. cereus* 16S rDNA sequencing was conducted using primers 7F and 1511R.

Table S3: List of plasmids used in this study

Plasmid	Genotype	Description
pAR5	*rpsB-mCherry-kan*	(Segev et al., 2013)
pGB10	*ymdB-gfp-spc*	Constructed by amplifying the *ymdB* from gDNA of wild type *B. subtilis* strain (PY79), using primers *ymdB*-U-*EcoR*I and *ymdB*-L-*Xho*I. The PCR-amplified DNA was digested with *EcoR*I and *Xho*I and was cloned into pKL147 (Lemon and Grossman, 1998) digested with the same enzymes.
pGB11	*amyE::*$P_{hyper\text{-}spank}$*-ymdB-spc*	Constructed by amplifying the *ymdB* from gDNA of *B. subtilis* strain (PY79), using primers *ymdB*-U-*Hind*III and *ymdB*-L-*Sph*I. The PCR-amplified DNA was digested with *Hind*III and *Sph*I and was cloned into pDR111 digested with the same enzymes. pDR111 is a gift from D. Rudner (Harvard U).
pGB13	*ymdB-gfp-kan*	Constructed by amplifying the 3' region of *ymdB* from genomic DNA of wild type *B. subtilis* strain (PY79), using primers *ymdB*-U-*EcoR*I and *ymdB*-L-*Xho*I. The PCR-amplified DNA was digested with *EcoR*I and *Xho*I and was cloned into pKL168 digested with the same enzymes.
pGB15	*ymdB-erm*	Constructed by amplifying the *ymdB* ORF genomic DNA of wild type *B subtilis* strain (PY79), using primers *ymdB-SDM*-U-*BamH*I and *ymdB-SDM*-L-*Hind*III. The PCR-amplified DNA was digested with *BamH*I and *Hind*III and was cloned into pMAD digested with the same enzymes.
pGB16	*ymdBD8A-erm*	Constructed by amplifying the *ymdB* ORF from pGB15, using primers *ymdB*-SDM8-U and *ymdB*-SDM8-L followed by *Dpn*I treatment for 1 hr to digest the methylated DNA template. Insert was sequenced to confirm the presence of the mutation.
pGB37	*amyE*::$P_{hyper\text{-}spank}$*-yjbK-spec*	Constructed by amplifying the *yjbK* ORF from genomic DNA of wild type *B. subtilis* strain (PY79), using primers *yjbK* -U-*Hind*III and *yjbK*-L-*Sph*I. The PCR-amplified DNA was digested with *Hind*III and *Sph*I and was cloned into pDR111 digested with the same enzymes.
pLS75	*malS-gfp-kan*	Constructed by amplifying the 3' region of *malS* from genomic DNA of wild type *B. subtilis* strain (PY79), using primers *malS*-U-*EcoR*I and *malS*-L-*Xho*I. The PCR-amplified DNA was digested with *EcoR*I and *Xho*I and was cloned into pKL168 digested with the same enzymes.

Table S4: List of primers used in this study

Primer Name	**Primer Sequence (5'-3')**
ecsB-ko –P1	TCCAGAACCCTGTCTCTTTATGACAG
ecsB-ko –P2	ACATGTATTCACGAACGAAAATCGAGGCCAGCGTCTTCCTTTGTAA
ecsB-ko –P3	ATTTTAGAAAACAATAAACCCTTGCAAAGCTGTGAACTGAAAAGAGGTAATC
ecsB-ko –P4	GGCGAGGATTTTGCTTATTACTTACA
hag- ko –P1	GAAAATACAATATACTCCGTCACAGC
hag- ko –P2	ATTATGTCTTTTGCGCAGTCGGCTGTTTTGTTCCTCCCTGAATATGTTG
hag- ko –P3	CATTCAATTTTGAGGGTTGCCAGTAATTTTAAAAAAGACCTTGGCGTTG
hag- ko –P4	CTGTTGTTTCGCCAGGCGCAAC
yqeK-ko –P1	TCTTTCCAATTGTGGACTGGACA
yqeK -ko –P2	ATCACCTCAAATGGTTCGCTGGGTTTCCATTCTCCTCTACATACTTCTTCACTT
yqeK -ko –P3	AAGTTCGCTAGATAGGGGTCCCGAGCAACAGGAGGAATTTGTGAATGAACC
yqeK -ko –P4	GTTCTTTGCTCGTGTGTCTCATC
ylbF-ko –P1	CAGATAAGGCCGTTTCCCATC
ylbF-ko –P2	GAACAACCTGCACCATTGCAAGAAACATGCACCTCCAGTTGTTAG
ylbF-ko –P3	TTGATCCTTTTTTTATAACAGGAATTCAGACTGGCCGTCTCGTCTTTTAC
ylbF-ko –P4	CGAATATACAATGCTCAAACCCGCG
yhxB-ko-P1	TGGGAACAACAGACACTGTTTAC
yhxB-ko-P2	ATCACCTCAAATGGTTCGCTGGGTTTCATATTCGTCCTCCTATGTATCAGC
yhxB-ko-P3	AAGTTCGCTAGATAGGGGTCCCGAGCTTCAAGTATGAGCTGGGTCATTG
yhxB-ko-P4	GCGCACCATAGCTTTTAATGG

yjbK::spc:-P1	CTTTTCTGGCAAAAAGCATCTCTTTTACG
yjbK::spc:-P2	CTGAGCGAGGGAGCAGAAGATGCTCTTCCTTTCCGCCCTGTAAATC
yjbK::spc:-P3	GTTGACCAGTGCTCCCTGTAAGGTGGAATGACATCGTGAATGTAAC
yjbK::spc:-P4	CTGACAGCCGGGGTTTGTATTTC
ymdB::tet-P1	GAGATGAAAGGACGTATCATCGGAC
ymdB::tet-P2	GAACAACCTGCACCATTGCAAGATTTGTAAATCCTTTCTTCTTGAAAATTCC
ymdB::tet-P3	TTGATCCTTTTTTTATAACAGGAATTCTAGTTGAACATATGGTTATTTTATAAAAATATTAAAAAG
ymdB::tet-P4	TGCTGACATTCTCTCCCACGCCCTC
ymdB-U-*EcoR*I	AAACCCGAATTCACATATGTGAAAGCAAACGGCAAAG
ymdB-L-*Xho*I	ACCTAGCTCGAGTTCAAGAACATGTGATCATCGTTG
ymdB-U-*HinD*III	AAACCCAAGCTTAAAGGTGGTGAACTACTATGAGAATTTTATTTATCGGAGATGTTGTC
ymdB-L-*Sph*I	ACCTAGGCATGCTTATTATTATTCAAGAACATGTGATCATCGTTG
ymdB-SDM-U-*BamH*I	AAACCCGGATCCGTAGAAGGAAGCCACGTTGAGATCGGGG
ymdB -SDM-L-*Hind*III	TAGTTTAAGCTTCTAAGGAGTTGCTATATTCCTGCTTTTC
ymdB-SDM8-U	GAATTTTATTTATCGGAGCTGTTGTCGGTTCACCGGG
ymdB-SDM8-L	CCCGGTGAACCGACAACAGCTCCGATAAATAAAATTC
yjbK -U-*Hind*III	GATCGAATTCCATGCTGACCAAACAAGAATTCAAAAAC
yjbK-L-*Sph*I	CCCAAACTCGAGTATAGACTTTCGTTTTTCTTCATAAAAACGC
malS-U-*EcoR*I	TGGACTGAATTCCCGCCAGTTGAATATAACGGAGTTAC
malS-L-*Xho*I	TGGACTCTCGAGTATCGCGCGAATCGGTTTGTATA

Supplemental Figure Legends

Figure S1, Related to Figure 1. Initiation morphologies of *B. subtilis* developing colonies

(**A**) A chamber allowing the visualization of a developing colony by CLSM. (I) Solid medium allowing bacterial growth. The developing colony grows over the bottom side of the solid surface. (II) A metal ring holding the solid medium. (III) A 1 mm thick silicon ring. The ring creates the 3D space between the media and the cover slip, essential for colony growth. (IV) A holding apparatus harboring a cover slip. The apparatus holds the components together and fits a standard Lab-Tek insert.

(**B**) An illustration of a cross section of the assembled components in A as well as the position of the growing colony and the microscope lens.

(**C**) *B. subtilis* spores expressing *rplA-gfp* (AR5) were diluted, plated on LB solid medium and incubated at 37°C. Fluorescence images were taken by CLSM at the indicated time points. Scale bars 5 μm.

(**D**) Cells of the undomesticated *B. subtilis* strain NCIB 3610 were diluted, plated on LB solid medium and incubated at 37°C. Transmitted light images were taken by CLSM at the indicated time points. Colony development was generally similar to the lab strain PY79, though the Y arms of 3610 developing colonies tend to branch more frequently. Scale bar 20 μm.

(**E**) Cells expressing P_{rrnE}-*gfp* (AR16) were diluted, plated on LB solid medium, incubated at 37°C, and colony formation was followed by CLSM. Shown are the three typical morphologies of developing colonies at stage I (t=3.5 hrs; upper panels) and at stage III (t=7 hrs; lower panels): Y shape- having three arms; Linear- having two arms; Multi branched- having at least 4 arms. Scale bar 10 μm.

Figure S2, Related to Figure 2. Tracking Y arm extension

(**A**) Cells (PY79) were diluted, plated on LB solid medium, incubated at 37°C, and colony formation was followed by CLSM. At the stage of Y shape formation, cells were irradiated at the indicated position of the single chained Y arm (red frame, arrow). The irradiated cells were marked by the addition of PI (red signal), and their location (highlighted by arrows) was tracked at the indicated time points. Shown are overlaid transmitted light and fluorescence images. Scale bars 20 μm.

(**B**) Cells expressing P_{rrnE}-*gfp* (AR16) were grown as described in A. At the stage of Y shape formation, cells at the tip of 2 single chained Y arms were irradiated, and the irradiated cells

were marked by the addition of PI (red signal). The calculated length of the non irradiated arm at 30 min was extended by 71%, while the length of the two irradiated arms increased by ~16% during that time. Shown are representative experiments out of 13 independent biological repeats. Scale bar 20 μm.

Figure S3, Related to Figure 4. YjbK is a potential adenylate cyclase in *B. subtilis*

(**A**) *ymdB-D8A-gfp* (GB201) cells were diluted, plated on LB solid medium and incubated at 37°C. Fluorescence images of two colonies at t=3.5 hrs, time corresponding to Y shape formation, exemplifying the aberrant morphologies. Scale bar 5 μm.

(**B**) Sequence alignment of the *B. subtilis* YjbK N-terminal region compared with the *E. coli* predicted adenylate cyclase YgiF, showing a clear homology of the CYTH domain. Based on database searches using PSI-BLAST and on reference (Iyer and Aravind, 2002).

(**C**) PY79 (wt), Δ*yjbK* (GB142), Δ*ymdB* (GB61) and Δ*ymdB* Δ*yjbK* (GB156), were grown on solid LB medium and incubated at 37°C for 20 hrs. Shown are typical colonies photographed using a binocular. Scale bar 0.5 mm.

(**D**) The average diameter of 20 colonies described in C.

(**E**) Distribution of each of the initial colony morphology patterns as described in Figure 1 for wild type (PY79) and Δ*yjbK* (GB142) strains. For each strain at least 100 colonies were scored.

(**F**) Intracellular cAMP level of 1 ml cells (OD_{600} 0.7 ~ $5x10^8$ cells/ml) of wild type (PY79) and Δ*yjbK* (GB142) strains grown in liquid medium as measured by ELISA assay.

(**G**) $P_{hyper\text{-}spank}$-*yjbK*, *ymdB-gfp* (GB222) cells were diluted, plated on LB solid medium with or without IPTG, incubated at 37°C and followed by time lapse microscopy. Fluorescence images were captured at the indicated time points post IPTG induction, and the GFP level of cells grown with or without IPTG was measured. Shown are the relative expression levels of YmdB-GFP with IPTG/ YmdB-GFP without IPTG (blue bars). As a control, a similar experiment was conducted with $P_{hyper\text{-}spank}$-*yjbK*, *malS- gfp* (GM13), expressing the unrelated GFP fusion to the metabolic enzyme MalS. MalS-GFP expression was not affected by over expressing YjbK. For each time point at least 50 cells were scored.

Figure S4, Related to Figure 5. Perturbing the formation of nanotube networks

(**A**) Δ*ymdB* (GB61) cells were diluted, plated on a thin layer of LB solid medium, incubated at 37°C and colony formation was followed by CLSM. At t=3.5 hrs cells were fixed, washed,

gold coated and observed with HR-SEM. A GB61 developing colony, exemplifying the abnormal morphology of the mutant colony. (1) Phase contrast image. (2) HR-SEM image of the same colony. (3) Magnification of the boxed region in 2.

(**B**) Cells expressing P_{rrnE}-*gfp* (AR16) were diluted, plated on LB solid medium, incubated at 37°C, and colony formation was followed by CLSM. At t=2 hrs the marked regions (red frames) were irradiated using 405 nm laser beam at full power (B_1). Next, the cells were fixed, washed, gold coated and observed with HR-SEM (B_2).

(**C**) High magnification images of the boxed regions in B_2 (1-3), and their interpretive cartoons illustrating nanotubes positions (white lines) and the irradiated area (red lines) (1'-3'). A clear difference in nanotube abundance can be seen between the irradiated and non-irradiated regions of the same cells.

Figure S5, Related to Figure 5. Testing the effect of irradiation and SDS addition on colony development

(**A**) Cells (PY79) were diluted, plated on LB solid medium containing PI, incubated at 37°C and colony formation was followed by CLSM. The red framed regions (cells or their surrounding area) were irradiated using 405 nm laser beam (left) and photographed 7 min later (right). Shown are overlaid transmitted light and fluorescence images. PI (red signal, right) was able to penetrate only the cells that were directly irradiated. Furthermore, cells that their surrounding area was irradiated continued to grow, indicating that they remained intact. Scale bar 10 μm.

(**B**) Intercellular regions distant from the center of a developing colony residing in stage I were irradiated using 405 nm laser beam (red frames). Shown are fluorescence images of a colony taken at the indicated time points. Red frames in t=4,5,6 hrs highlight the area irradiated at t=3.5 hrs. Scale bar 20 μm.

(**C**) Fluorescent dyes (FM1-43, PI, Acrydin Orange) were added to LB agar and a marked region (30 μm^2) was bleached using 405 nm laser beam. Shown are FRAP charts of the 3 different fluorescent stains from areas located at the indicated distances from the center of the irradiated region (0 μm). The quick recovery of the fluorescent signal indicates that small molecules are rapidly diffused through the agar.

(**D**) Cells expressing P_{rrnE}-*gfp* (AR16) were diluted, plated on LB solid medium containing 0.007% SDS, incubated at 37°C, and colony formation was followed by CLSM. Shown are

two representative examples of developing colonies at t=3.5 hrs of development. Scale bar 10 μm.

Supplemental Movie Legends

Movie S1, Related to Figure 1. Y shape formation

Time lapse images of Y shape formation. Cells expressing P_{rrnE}-*gfp* (AR16) were diluted, plated on LB solid medium and incubated at 37°C in a 2D construct. Fluorescence images were taken by CLSM using 100X immersion lens at 12 min intervals in the course of 2 hrs.

Movie S2, Related to Figure 2. *B. subtilis* colony development

Time lapse images of colony development. Cells expressing P_{rrnE}-*gfp* (AR16) were diluted, plated on LB solid medium and incubated at 37°C. Fluorescence images were taken by CLSM at 15 min intervals in the course of 8 hrs.

Movie S3, Related to Figure 3. Irradiating one arm leads to asymmetric colony growth

Time lapse images of colony development following Y arm eradication. Cells expressing P_{rrnE}-*gfp* (AR16) were diluted, plated on LB solid medium and incubated at 37°C. At t= 3 hrs one arm of the developing colony was irradiated using 405 nm laser. Fluorescence images were taken by CLSM at 20 min intervals in the course of 6 hrs.

Movie S4, Related to Figure 5. *B. subtilis* colony development on SDS containing medium

Time lapse images of colony development. Cells expressing P_{rrnE}-*gfp* (AR16) were diluted, plated on LB solid medium supplemented with 0.007% SDS and incubated at 37°C. Fluorescence images were taken by CLSM at 20 min intervals in the course of 3.5 hrs.

Movie S5, Related to Figure 2. *B. cereus* colony development

Time lapse images of *B. cereus* colony development. *B. cereus* cells were diluted, plated on LB solid medium and incubated at 37°C. Transmitted light microscopy images were taken by CLSM at 20 min intervals in the course of 6 hrs.

Supplemental Experimental Procedures

General Methods

All general methods were carried out as described previously (Harwood and Cutting, 1990). For colony development experiments, growth was carried out at 37°C. Cells were incubated in liquid Luria Broth (LB) medium at 23°C overnight, and diluted to cell density of approximately 1 cell/μl (accordingly, a typical start up culture of OD_{600} 0.7 was diluted up to 10^{-5}). Isopropyl β-D-1-thiogalactopyranoside (IPTG) was added to a final concentration of 1 mM, when indicated. Sodium dodecyl sulfate (SDS) was added to a final concentration of 0.007% when indicated. Mature colonies grown overnight on LB plates were observed and photographed using Discovery V20 steroscope (Zeiss) equipped with Infinity1 camera (Luminera). Sporulation was induced by suspending cells in Schaeffer's liquid medium (DSM) (Schaeffer et al., 1965).

Measuring the Radial Area Occupied by a Developing Colony

Calculating the radial area occupied by a given colony was carried out by measuring the area of the minimal circle harboring the entire population of cells at the analyzed stage. The measured area was then normalized to the total number of cells in the developing colony, as estimated by measuring the total chain length. For *ymdB* mutant cells the area of at least 12 developing colonies was averaged and compared with the averaged area of 12 wild type colonies grown side by side.

Testing Diffusion Rates of Small Molecules on Agarose Pads

LB agarose pad (1.5%) was supplemented with the fluorescent dyes FM 1-43 (3 μg/ml) (Invitrogene), PI (20 μg/ml) (Sigma) or Acrydin Orange (40 μg/ml) (Sigma). A circled region (30 μm^2) was bleached at the center of the field using 405 nm laser at full power (5 mW, 75 iterations). Fluorescence levels from areas surrounding the bleached region at different distances were monitored every 0.5 min for 2.5 min.

cAMP ELISA Test

Enzyme-Linked Immunosorbent Assay (ELISA) test was conducted using Direct cAMP ELISA kit (ENZO Life Sciences). Cells were grown in liquid LB at 23°C over night. For each tested strain, 4 ml of the liquid culture (OD_{600} 0.7, ~$5x10^8$ cells/ml) were centrifuged

and the liquid fraction was decanted. Cells were washed with PBSx1, centrifuged and suspended in 125 µl of 1.8 mg/ml lysozyme, and incubated at 37°C. After 30 min, 125 µl of 0.2 M HCl were added and samples were incubated at room temperature for 15 min. Next, 20 µl sample were taken for Bradford assay to normalize the total protein concentration, and 25 µl of 10% Triton X-100 were added to the remaining samples. Samples were incubated at room temperature for 20 min and then tested for uniformity of cell lysis with phase contrast microscopy. Next, samples were centrifuged at 800 rpm and the supernatant was taken for ELISA analysis according to the manufacturer protocol. In order to get high sensitivity of the assay the acetylated protocol was used. cAMP levels were calculated per 1 ml cell culture.

Supplemental References

Harwood, C.R., and Cutting, S.M. (1990). Molecular biological methods for *Bacillus*. In Modern microbiological methods (Chichester ; New York: Wiley,).

Ireton, K., Rudner, D.Z., Siranosian, K.J., and Grossman, A.D. (1993). Integration of Multiple Developmental Signals in *Bacillus subtilis* through the Spo0A Transcription Factor. Genes Dev *7*, 283-294.

Lei, Y., Oshima, T., Ogasawara, N., and Ishikawa, S. (2013). Functional analysis of the protein Veg, which stimulates biofilm formation in *Bacillus subtilis*. J Bacteriol *195*, 1697-1705.

Lemon, K.P., and Grossman, A.D. (1998). Localization of bacterial DNA polymerase: evidence for a factory model of replication. Science *282*, 1516-1519.

Mirel, D.B., and Chamberlin, M.J. (1989). The *Bacillus subtilis* flagellin gene (hag) is transcribed by the sigma 28 form of RNA polymerase. J Bacteriol *171*, 3095-3101.

Rosenberg, A., Sinai, L., Smith, Y., and Ben-Yehuda, S. (2012). Dynamic expression of the translational machinery during *Bacillus subtilis* life cycle at a single cell level. PLoS One *7*, e41921.

Schaeffer, P., Millet, J., and Aubert, J.P. (1965). Catabolic repression of bacterial sporulation. Proc Natl Acad Sci U S A *54*, 704-711.

Segev, E., Rosenberg, A., Mamou, G., Sinai, L., and Ben-Yehuda, S. (2013). Molecular Kinetics of Reviving Bacterial Spores. J Bacteriol *195*, 1875-1882.

Serrano, M., Zilhao, R., Ricca, E., Ozin, A.J., Moran, C.P., and Henriques, A.O. (1999). A *Bacillus subtilis* secreted protein with a role in endospore coat assembly and function. J Bacteriol *181*, 3632-3643.

Tortosa, P., Albano, M., and Dubnau, D. (2000). Characterization of *ylbF*, a new gene involved in competence development and sporulation in *Bacillus subtilis*. Mol Microbiol *35*, 1110-1119.

Youngman, P., Perkins, J.B., and Losick, R. (1984). Construction of a cloning site near one end of Tn917 into which foreign DNA may be inserted without affecting transposition in *Bacillus subtilis* or expression of the transposon-borne *erm* gene. Plasmid *12*, 1-9.